

# Highly Predictive Transdiagnostic Features Shared across Schizophrenia, Bipolar Disorder, and ADHD Identified Using a Machine Learning Based Approach

1 Yuelu Liu<sup>1</sup>, Monika S. Mellem<sup>1</sup>, Humberto Gonzalez<sup>1</sup>, Matthew Kollada<sup>1</sup>, Atul R.  
2 Mahableshwarkar<sup>1</sup>, Annette Madrid<sup>1</sup>, William J. Martin<sup>1</sup>, Parvez Ahammad<sup>1\*</sup>

3 <sup>1</sup>Blackthorn Therapeutics, Inc., San Francisco, CA, USA

4 \* **Correspondence:**

5 Parvez Ahammad, PhD

6 parvez.ahammad@blackthornrx.com

7 **Keywords:** transdiagnostic, schizophrenia, bipolar disorder, ADHD, machine learning.

8 **Abstract**

9 The Diagnostic and Statistical Manual of Mental Disorders (DSM) has been the standard for  
10 diagnosing psychiatric disorders in the United States. Yet, evidence has suggested that symptoms in  
11 psychiatric disorders are not restricted to the boundaries between DSM categories, implicating an  
12 underlying latent transdiagnostic structure of psychopathology. Here, we applied an importance-  
13 guided machine learning technique for model selection to item-level data from self-reported  
14 instruments contained within the Consortium for Neuropsychiatric Phenomics dataset. From 578  
15 questionnaire items, we identified a set of phenotypic features which consisted of 85 items that were  
16 shared across diagnoses of schizophrenia (SCZ), bipolar disorder (BD), and attention  
17 deficit/hyperactivity disorder (ADHD). A transdiagnostic classifier trained on the shared phenotypic  
18 features reliably distinguished the patient group as a whole from healthy controls (classification AUC  
19 = 0.95) and only 10 items were needed to attain the performance level of AUC being 0.90. A sum  
20 score created from the items produced high separability between patients and healthy controls  
21 (Cohen's  $d = 2.85$ ), and it outperformed predefined sum scores and sub-scores within the instruments  
22 (Cohen's  $d$  ranging between 0.13 and 1.21). The shared phenotypic features comprised both  
23 symptom domains (e.g. dysregulated mood, attention deficits, and impaired reward processing) and  
24 personality traits (e.g. neuroticism, impulsivity, and extraversion). Moreover, by comparing these  
25 features with those that were most predictive of a single patient category, we can describe the unique  
26 features for each patient group superimposed on the transdiagnostic feature structure. Overall, our  
27 results reveal a latent transdiagnostic phenotypic structure shared across SCZ, BD, and ADHD and  
28 present a new perspective to understand insights offered by self-report psychiatric instruments.

29 **Number of words:** 5644

30 **Number of words in abstract:** 265

31 **Number of figures:** 4

## 32 1 Introduction

33 The Diagnostic and Statistical Manual of Mental Disorders (DSM) provides a symptom-based  
34 taxonomy which serves to help clinicians classify various clusters of symptoms and abnormal  
35 behaviors into distinct categories of disorders. The uniformity of diagnostic criteria in DSM serves to  
36 effectively index psychiatric disorders but does not provide a data-driven framework within which to  
37 understand the shared and unique features across disorders. For example, dimensionality and  
38 comorbidity are pervasive in terms of symptoms across different DSM categories (Kessler et al.,  
39 2005; Markon, 2009; Krueger and Markon, 2011). Such dimensionality manifests as heterogeneity in  
40 symptom clusters within disease categories defined by the DSM and is exemplified across DSM  
41 categories (Kessler et al., 2007). In the area of anxiety and mood disorders, more than 50% of  
42 individuals are diagnosed as having more than a single category of disorders according to the DSM at  
43 a given time (Grisanzio et al., 2017). Similarly, about 50% of bipolar disorder patients exhibit  
44 schizophrenia-like psychotic symptoms during illness episodes (Coryell et al., 2001; Keck et al.,  
45 2003). The presence of such psychotic symptoms can be mood-incongruent (Pacheco et al., 2010)  
46 and can occur outside of illness episodes (Pope and Lipinski, 1978; Abrams and Taylor, 1981). These  
47 observations highlight the likelihood of a latent trans-diagnostic dimensional structure that spans  
48 multiple disorders (Krueger and Markon, 2006) and underscore the importance of understanding  
49 patients at the symptom-level, rather than simply at a diagnostic level, to create more effective  
50 treatments.

51 Studies have attempted to uncover the latent structure of psychopathology, between or within  
52 categories, through multimodal assessments that measure symptoms, behavior, physiology, imaging,  
53 and genetics. One such example is the large-scale study conducted by the UCLA Consortium for  
54 Neuropsychiatric Phenomics (CNP), which seeks to identify links among phenotypic data, imaging,  
55 and genetics (Poldrack et al., 2016). Overall, genetic studies have pointed to the heritability of major  
56 neuropsychiatric disorders (Cross-Disorder Group of the Psychiatric Genomics Consortium, 2013;  
57 Hamshere et al., 2013; Larsson et al., 2013; The Brainstorm Consortium et al., 2017; Bipolar  
58 Disorder and Schizophrenia Working Group of the Psychiatric Genomics Consortium et al., 2018;  
59 Gandal et al., 2018) as well as the genetic commonality amongst disorders (Purcell et al., 2009; Lotan  
60 et al., 2014) such as schizophrenia (SCZ), bipolar disorder (BD), and attention deficit/hyperactivity  
61 disorder (ADHD). Recent data-driven studies based on symptom and behavior have focused on  
62 classifying and subtyping patients within a single diagnostic category (Lamers et al., 2012; van Loo  
63 et al., 2012; Georgiades et al., 2013; Doshi-Velez et al., 2014; van Hulst et al., 2014; Costa Dias et  
64 al., 2015; Geisler et al., 2015; Sun et al., 2015; Drysdale et al., 2016; Gheiratmand et al., 2017).  
65 Several of these studies identified important shared abnormal features associated with the latent  
66 transdiagnostic structure across major psychiatric disorders.

67 The clinical utility of using the features identified in the above-mentioned studies to reliably classify  
68 patients remains an open question. Emerging studies have used unsupervised machine learning  
69 approaches, such as clustering and dimensionality reduction algorithms, to uncover the  
70 transdiagnostic structure across disorders (Grisanzio et al., 2017; Xia et al., 2018). However, the lack  
71 of ground truth on how patients should be assigned to an identified cluster/subtype limits the  
72 application of these insights. Moreover, because studies did not adopt a supervised machine learning  
73 predictive framework wherein the identified features along with the predictive algorithms are  
74 rigorously tested on unseen data to mimic real-world clinical diagnostics, the validity of these  
75 transdiagnostic subtypes is yet to be fully established.

76 In the current study, we take a patient-focused approach to identify transdiagnostic features that are  
77 shared across SCZ, BD, and ADHD derived from self-reported responses on clinically-accepted  
78 questionnaires. Using an importance-guided model selection approach, the supervised machine  
79 learning framework used in this study allowed us to evaluate the performance of the transdiagnostic  
80 features and hence to iteratively identify the optimal set of features required to distinguish the patient  
81 group from healthy controls (HCs). Based on the CNP dataset, we used multiple data modalities  
82 including the behavioral/symptom phenotypes (from here on referred to as phenotypes) defined in  
83 self-reported instruments and neuroimaging data (sMRI and fMRI) to obtain the optimal  
84 transdiagnostic features. We then report these shared features and discuss the identified latent  
85 psychopathological structure across these psychiatric disorders.

86

## 87 **2 Materials and Methods**

### 88 **2.1 The CNP dataset**

89 We utilized the openly available dataset from the CNP LA5c Study conducted at the University of  
90 California, Los Angeles (the CNP dataset: <https://openneuro.org/datasets/ds000030/versions/00016>).  
91 Detailed information on the CNP study/dataset can be found in (Poldrack et al., 2016). The CNP  
92 dataset contains a variety of data modalities. In this study, we focused on identifying shared  
93 transdiagnostic features based on the item-level data from self-reported instruments as well as  
94 neuroimaging data (including both sMRI and resting-state fMRI). The dataset in this study includes  
95 272 subjects, of which 50 are diagnosed with schizophrenia (SCZ), 49 with bipolar disorder (BD),  
96 and 43 with attention deficit/hyperactivity disorder (ADHD). The remaining 130 subjects are age-  
97 matched healthy controls (HC). The diagnoses were given by following the Diagnostic and Statistical  
98 Manual of Mental Disorders, Fourth Edition, Text Revision (DSM-IV-TR; American Psychiatric  
99 Association, 2000) and were based on the Structured Clinical Interview for DSM-IV (First et al.,  
100 2002). To better characterize ADHD related symptoms, the Adult ADHD Interview (Kaufman et al.,  
101 2000) was further used as a supplement. Out of all subjects, 1 had incomplete phenotype data from  
102 the instruments used in this study, 10 had missing structural MRI (sMRI) data, and 10 had missing  
103 resting-state functional MRI (fMRI) data. Fifty-five (55) subjects had an aliasing artifact in their  
104 sMRI data potentially caused by the headset used in the scanner, whereas 22 subjects had errors in  
105 the structural-functional alignment step during MRI preprocessing. These subjects were excluded  
106 from the corresponding modeling analyses performed in this study. The subject numbers and  
107 demographics information are given in **Table 1**.

### 108 **2.2 Phenotype data**

109 Subjects were administered a total of 20 clinical instruments to capture a wide range of phenotype  
110 data including specific behavioral traits and symptom dimensions (Poldrack et al., 2016). These  
111 instruments are either clinician-rated or self-reported. While the clinician-rated questionnaires only  
112 covered relevant patient groups, 13 self-reported clinical scales were given to all three patient groups  
113 as well as the healthy controls. We therefore used subjects' answers to each of the individual  
114 questions coming from these 13 self-reported scales as input features to our models. Specifically, the  
115 13 self-reported scales used in this study are: Chapman Social Anhedonia Scale, Chapman Physical  
116 Anhedonia Scale, Chapman Perceptual Aberrations Scale, Hypomanic Personality Scale, Hopkins  
117 Symptom Checklist, Temperament and Character Inventory, Adult ADHD Self-Report Scale v1.1  
118 Screener, Barratt Impulsiveness Scale, Dickman Functional and Dysfunctional Impulsivity Scale,  
119 Multidimensional Personality Questionnaire – Control Subscale, Eysenck's Impulsivity Inventory,

120 Scale for Traits that Increase Risk for Bipolar II Disorder, and Golden and Meehl's Seven MMPI  
121 Items Selected by Taxonomic Method.

## 122 **2.3 MRI data acquisition parameters**

123 MRI data were acquired on one of two 3T Siemens Trio scanners both housed at the University of  
124 California, Los Angeles. The sMRI data used in this study are T1-weighted and were acquired using  
125 a magnetization-prepared rapid gradient-echo (MPRAGE) sequence with the following acquisition  
126 parameters: TR = 1.9 s, TE = 2.26 ms, FOV = 250 mm, matrix = 256 x 256, 176 1-mm thick slices  
127 oriented along the sagittal plane. The resting-state fMRI data contain a single run lasting 304 s. The  
128 scan was acquired using a T2\*-weighted echoplanar imaging (EPI) sequence using the following  
129 parameters: 34 oblique slices, slice thickness = 4 mm, TR = 2 s, TE = 30 ms, flip angle = 90°, matrix  
130 size 64 x 64, FOV = 192 mm. During the resting-state scan, subjects remained still and relaxed inside  
131 the scanner, and kept their eyes open. No specific stimulus or task was presented to them.

## 132 **2.4 MRI preprocessing**

### 133 **2.4.1 sMRI**

134 Structural MRI preprocessing was implemented using Freesurfer's *recon-all* processing pipeline  
135 (<http://surfer.nmr.mgh.harvard.edu/>). Briefly, the T1-weighted structural image from each subject  
136 was intensity normalized and skull-stripped. The subcortical structures, white matter, and ventricles  
137 were segmented and labeled according to the algorithm described in (Fischl et al., 2002). The pial  
138 and white matter surfaces were then extracted and tessellated (Fischl et al., 2001), and cortical  
139 parcellation was obtained on the surfaces according to a gyral-based anatomical atlas which partitions  
140 each hemisphere into 34 regions (Desikan et al., 2006).

### 141 **2.4.2 Resting-state fMRI**

142 Resting-state fMRI preprocessing was implemented in AFNI (<http://afni.nimh.nih.gov/afni/>).  
143 Specifically, the first 3 volumes in the data were discarded to remove any transient magnetization  
144 effects in the data. Spikes in the resting-state fMRI data were then removed and all volumes were  
145 spatially registered with the 4<sup>th</sup> volume to correct for any head motion. The T1w structural image was  
146 deobliqued and uniformized to remove shading artifacts before skull-stripping. The skull-stripped  
147 structural image was then spatially registered with motion corrected fMRI data. The fMRI data were  
148 further spatially smoothed using a 6-mm FWHM Gaussian kernel and converted to percent signal  
149 change. Separately, the Freesurfer-generated *aparc+aseg* image from sMRI preprocessing was also  
150 spatially registered with and resampled to have the same spatial resolution of the BOLD image.  
151 Based on this, eroded white matter and ventricle masks were created, from which nuisance tissue  
152 regressors were built based on non-spatially smoothed fMRI data to model and remove variances that  
153 are not part of the BOLD signal. Specifically, we used the ANATICOR procedure (Jo et al., 2010),  
154 where a locally averaged signal from the eroded white matter mask within a 25-mm radius spherical  
155 region of interest (ROI) centered at each gray matter voxel was used to create a voxel-wise local  
156 estimate of the white matter nuisance signal. This local estimate of the white matter nuisance signal,  
157 along with the estimated head motions and average signal from the ventricles were detrended with a  
158 4<sup>th</sup> order polynomial and then regressed out from the fMRI data. Finally, the clean resting-state fMRI  
159 data was spatially normalized to the MNI template and resampled to have 2 mm isotropic voxels.

## 160 **2.5 Feature extraction**

161 We extracted measures from 3 data modalities as features: phenotype data from self-reported  
162 instruments, measures derived from the sMRI data, and functional correlations based on resting-state  
163 fMRI data. For phenotype features from self-reported instruments, we directly used subjects'  
164 responses from a total of 578 questions from the above listed 13 instruments. Responses from non-  
165 True/False type questions were normalized to have a range of between 0 and 1 to match those from  
166 True/False type questions. For sMRI features, we specifically used 1) the volume of subcortical  
167 structures generated by Freesurfer's subcortical volumetric segmentation, and 2) the area, thickness,  
168 and volume of cortical brain regions estimated from Freesurfer's surface-based analysis pipeline. For  
169 resting-state fMRI features, we first parceled the brain into 264 regions according to the atlas  
170 proposed in (Power et al., 2011). A 5-mm radius spherical ROI was seeded according to the MNI  
171 coordinates of each brain region specified in the atlas. Second, the clean resting-state BOLD time  
172 series from all voxels within a given 5-mm radius spherical ROI were averaged to create the  
173 representative time series for the brain region. Third, functional connectivity between ROIs was  
174 estimated via the Pearson's correlation coefficient between the average time series from all pairs of  
175 brain regions. This produced a 264-by-264 correlation matrix, from which 34,716 are unique  
176 correlations between two distinct ROIs and were used as input features to the models.

## 177 **2.6 Model fitting and feature importance weighting**

178 The primary goals of machine learning analyses in this study were two-fold: 1) to identify important  
179 features commonly found across patient groups and 2) to establish robust transdiagnostic classifiers  
180 that can reliably separate patient groups from healthy controls. To achieve these goals, we built  
181 transdiagnostic classifiers based on the logistic regression model as implemented in the *scikit-learn*  
182 toolbox to classify patients from HCs. To identify predictive transdiagnostic features embedded  
183 within each feature modality, separate logistic regression models were independently trained using  
184 each of the above extracted feature modalities (i.e., item-level phenotype data, sMRI measures, and  
185 resting-state fMRI correlations) as inputs and their performances were evaluated in each of the  
186 transdiagnostic scenarios. Combinations of 2 and 3 feature modalities were also used as classifiers'  
187 inputs and their performances were evaluated in the same fashion.

188 Because the number of features we extracted was relatively large compared to the sample size in  
189 CNP data, an elastic net regularization term (Zou and Hastie, 2005) was added in all of our logistic  
190 regression models to prevent overfitting. The use of elastic net regularization in our models also  
191 enabled feature selection as the regularization induces sparse models via the grouping effect where  
192 all the important features will be retained and the unimportant ones set to zero (Zou and Hastie, 2005;  
193 Ryali et al., 2012). This allowed us to identify predictive features that are shared across multiple  
194 patient categories.

195 We adopted the following procedure to determine the best regularization parameters. First, the input  
196 data were randomly partitioned into a development set and an evaluation set. The development set  
197 contains 80% of the data upon which a grid search with 3-fold cross validation procedure was  
198 implemented to determine the best regularization parameters. Then the model with the best  
199 regularization parameters was further tested on the remaining 20% of evaluation set. All features  
200 were standardized to have zero mean and unit variance within the training data and the mean and  
201 variance from the training data were used to standardize the corresponding test data. The entire  
202 process was implemented 10 times. The following metrics were used to quantify the model  
203 performances: area under the receiver operating characteristics curve (AUC), accuracy, sensitivity,  
204 and specificity. The mean and standard deviation of the above metrics over the 10 evaluation sets  
205 were reported.

206 From the above models, the predictive power of each feature is assessed via the weights of the  
207 logistic regression model in our transdiagnostic classifiers. For each feature, we calculated its  
208 corresponding standardized model weight (mean model weight divided by the standard deviation)  
209 across the 10 model implementations as the proxy for feature importance. Features with large  
210 importance values from our transdiagnostic classifiers are potentially symptoms, traits, and  
211 neuropathological mechanisms shared across patient groups but are distinct from healthy controls.

212 To identify the set of most predictive transdiagnostic features within a given data modality, we used  
213 the following feature importance-guided sequential model selection procedure. Specifically, we first  
214 rank ordered the features in the transdiagnostic classifiers according to their standardized model  
215 weights. Next, a series of truncated models was built such that each model only takes the top k most  
216 predictive features as inputs to perform the same transdiagnostic classification tasks. We let k range  
217 from the top 1 most predictive feature to all available features in steps of 1 for phenotype features,  
218 sMRI features, and the combination of the two feature sets. For any feature or feature combinations  
219 involving fMRI correlations, because of the significantly increased feature dimension, the k's were  
220 chosen from a geometric sequence with a common ratio of 2 (i.e., 1, 2, 4, 8, 16, ...). Model  
221 performances were obtained for each truncated model and were evaluated as a function of the number  
222 of top features (k) included in each truncated model to determine the optimal feature set.

## 223 2.7 Statistical analyses

224 To statistically examine whether the models' performances are significantly above chance level, we  
225 performed a random permutation test where labels in the training data (e.g., HC vs. Patients) were  
226 shuffled 100 times and truncated models based on the best set of features were trained on these label-  
227 shuffled data using exactly the same approach as described above (Ojala and Garriga, 2009). The  
228 performances from the 100 models were used to construct the empirical null distribution against  
229 which the performance of the best truncated models based on the actual unshuffled data was then  
230 compared. This random permutation test procedure also helped us to determine whether overfitting  
231 occurred during training.

232 To evaluate differences in sum scores obtained from the top features between HC and patients, we  
233 used two sample t-tests on the sample means since the sum scores are quasi normally distributed.  
234 Effect sizes were measured using Cohen's d, which captures the shift in mean scaled by the data's  
235 standard deviation. Tests on the difference in AUC between the full model and the best truncated  
236 model were carried out via the Wilcoxon's rank-sum test.

237

## 238 3 Results

239 In total, the HC vs. patients transdiagnostic classifiers were trained and tested on 7 sets of features by  
240 either using each individual feature modality (self-reported instruments, sMRI, and fMRI) or  
241 combinations of 2 or 3 feature modalities (e.g., instruments+sMRI+fMRI). The classifiers'  
242 performances using each of the 7 feature sets for the HC vs. Patients transdiagnostic cases are  
243 reported in **Table 2**. Overall, classifiers trained on feature sets involving phenotypical data from self-  
244 reported instruments (i.e., scales and scales + MRI feature sets) outperformed those only trained on  
245 MRI features (sMRI, fMRI, and sMRI+fMRI). For classifiers using features involving these  
246 instruments, the mean AUC ranged from 0.83 to 0.89 (mean accuracy: 0.77 – 0.91), whereas the  
247 mean AUC ranged from 0.56 to 0.59 (mean accuracy: 0.58 – 0.61) for MRI feature sets.

248 Next, to identify the optimal set of shared features among patients that are highly distinct from HC,  
249 we examined the performance measures from the best truncated classification models during  
250 sequential model selection (**Figure 1** and **Table 2**; see **Supplementary Fig. 1** for AUC as a function  
251 of input feature dimensions). Significantly improved performances were obtained from the best  
252 truncated classification models compared with the corresponding models using the full sets of  
253 features (all  $p$ 's  $< 0.05$  as assessed by the rank-sum test; **Table 2**). The AUCs from all feature sets  
254 were also significantly above chance level as assessed via the random permutation test (all  $p$ 's  $<$   
255  $0.05$ ; **Supplementary Fig. 2**). Additionally, the computational time for the importance guided  
256 sequential model selection method grew linearly as the number of features increased, which is highly  
257 efficient compared to the brute force feature selection procedure (exponential time complexity;  
258 **Supplementary Fig. 3**).

259 The truncated classification model involving data from the self-reported instruments alone had high  
260 performance of distinguishing patients from HCs with the mean AUC being 0.95 (accuracy: 0.88;  
261 sensitivity: 0.87; specificity: 0.88; **Figure 1**; **Table 2**). This truncated model selected 85 items as the  
262 most predictive features from the total of 578 items contained in the 13 self-reported instruments.  
263 Moreover, only 10 items were needed to achieve an AUC of 0.90 (accuracy: 0.81; sensitivity: 0.79;  
264 specificity: 0.84), suggesting that a concise scale can be constructed potentially for screening  
265 purposes. The model involving data from self-reported instruments performed better compared to  
266 those using feature sets based solely on MRI (mean AUC ranging from 0.77 to 0.87; mean accuracy  
267 ranging from 0.71 to 0.85). Combining MRI features with data from instruments only slightly  
268 improved the model performance (mean AUC being 0.96 – 0.98) (**Figure 1**; **Table 2**). Taken  
269 together, this indicates that the phenotypical data captured by the 13 self-reported instruments contain  
270 a set of transdiagnostic features that are common across the patient populations and, at the same time,  
271 are highly distinct from healthy controls. We hence focused on discussing these transdiagnostic  
272 phenotypical features below.

273 A simple sum score constructed by adding up an individual's responses to the 85 most predictive  
274 items (with item responses having negative model coefficients reversed) demonstrated high  
275 separability between healthy controls and patients (Cohen's  $d = 2.85$ ; test on the difference in sample  
276 mean:  $t = 10.27$ ,  $p < 0.001$ ; **Figure 2A**). The separability based on the top 10 most predictive items  
277 (corresponding AUC = 0.90) was also very high (Cohen's  $d = 2.16$ ; test on the difference in sample  
278 mean:  $t = 18.13$ ,  $p < 0.001$ ). The sum scores had higher separability than other known sum  
279 scores/sub-scores of the self-reported instruments (**Figure 2C & 2D**; **Supplementary Table 1**),  
280 indicating the items selected by the transdiagnostic classifier do not adhere to known dimensional  
281 structures within the instruments. Calculating the sum score for each individual patient category  
282 showed that all 3 patient categories had elevated sum scores compared to healthy controls ( $t > 5.671$ ,  
283  $p < 0.001$ ); yet, the difference between the patient categories was insignificant ( $t < 1.940$ ,  $p > 0.056$ ;  
284 **Figure 2B**). This suggests that the 85 items captured transdiagnostic phenotypic features shared  
285 across the patient groups as a whole rather than driven by a single patient category.

286 **Figure 3** illustrates the proportion of questionnaire items selected from each instrument that were  
287 included in transdiagnostic set of phenotypic features of the best truncated model (i.e. the one with  
288 the highest AUC). Items from all 13 instruments were selected to be among the top features by the  
289 classifiers. Overall, these instruments measure a wide range of phenotype and symptom domains  
290 encompassing personality traits, positive and negative affect (reward/anhedonia, fear, and anxiety),  
291 cognition (attention, response inhibition), sensory processing (perceptual disturbances), and social  
292 processing. While all items included among the set of transdiagnostic phenotypic features jointly  
293 formed a highly predictive set to distinguish patients from healthy controls, the Temperament and

294 Character Inventory (TCI) contributed the largest proportion of items in the transdiagnostic classifier.  
295 The proportion of TCI items selected among the 85 most predictive items (32.9%) significantly  
296 exceeded the proportion of all TCI items among all 578 items from the 13 instruments (24.0%;  $p =$   
297 0.04 as assessed via the Z-test). The disproportionately high number of TCI items indicates that  
298 certain personality traits are strong predictors of shared psychopathology regarding SCZ, BD, and  
299 ADHD.

300 To better understand which features strongly predicted psychopathology, we focused on the top 20  
301 items that contributed the largest magnitude of model weights. Among personality traits, the top  
302 transdiagnostic features included neuroticism, extraversion, and impulsivity (**Figure 4A**); whereas  
303 the top symptom domains consisted of mood dysregulation, inattention, hyperactivity/agitation, and  
304 social anhedonia and apathy. In addition, the importance of religion was also a shared feature across  
305 patients (**Figure 4A**; see **Supplementary Table 3** for item grouping). We next compared the most  
306 predictive transdiagnostic features with those most predictive of a single patient category from  
307 healthy controls to identify category-specific differences (**Figure 4B-D**; see **Supplementary Table 2**  
308 **and Supplementary Fig. 4** for classification results between HC and each patient category). SCZ  
309 patients exhibited additional features including perceptual aberration, physical anhedonia, and  
310 psychological distress that are not among the top transdiagnostic features. On the other hand,  
311 extraversion, impulsivity, inattention, and religion which were present in the transdiagnostic features  
312 set were not among the most predictive features for SCZ (**Figure 4B** and **Supplementary Table 4**).  
313 By contrast, transdiagnostic features overlapped with BD patient-specific features. Nonetheless, BD  
314 patients exhibited additional features of increased energy, psychological distress and physical  
315 anhedonia; yet psychomotor agitation and neuroticism contributed little predictive value (**Figure 4C**,  
316 **Supplementary Table 5**). ADHD patients were effectively classified by additional features such as  
317 indecision and physical anhedonia, with little predictive contribution from apathy, neuroticism, and  
318 religion (**Figure 4D**, **Supplementary Table 6**).

319

## 320 4 Discussion

321 In this study, using self-reported instruments provided in the CNP dataset, we generated predictive  
322 models to identify a set of transdiagnostic phenotypic features that were shared across SCZ, BD, and  
323 ADHD. These models were quantified for performance (e.g. accuracy, sensitivity and specificity) and  
324 were interpretable along dimensions of personality traits and symptom domains. We found the set of  
325 85 items is highly predictive of the patient group as a whole from HCs. To our surprise, a compact  
326 model of only 10 items is sufficient to achieve a performance AUC value of 0.90. Further, we  
327 demonstrated that a simple sum score can be calculated to enable high separability between patients  
328 and HCs. Our importance-guided sequential model selection approach revealed which phenotypical  
329 features were shared across transdiagnostic patient groups. Within each patient population, we also  
330 show which abnormal psychopathological personality traits and symptom domains deviated from the  
331 transdiagnostic classifier. Importantly, many of these features are consistent with established clinical  
332 intuition. Taken together, this study offers new perspectives on the shared psychopathology across  
333 SCZ, BD, and ADHD and underscores the potential of creating a short transdiagnostic screening  
334 scale based on the selected items.

335 The application of machine learning to systematically search for consistent patterns in clinical data  
336 across disease categories defined in DSM is an emerging trend in the field of computational  
337 psychiatry (Bzdok and Meyer-Lindenberg, 2017). Nonetheless, our approach to identifying



338 transdiagnostic features in psychiatric disorders differs both conceptually and methodologically from  
339 previous studies. Numerous investigators have focused on patient subtyping within a given disorder  
340 (Rhebergen et al., 2011; Lamers et al., 2012; van Loo et al., 2012, 2014; Georgiades et al., 2013;  
341 Brodersen et al., 2014; Doshi-Velez et al., 2014; Lewandowski et al., 2014; van Hulst et al., 2014;  
342 Veatch et al., 2014; Costa Dias et al., 2015; Geisler et al., 2015; Sun et al., 2015; Clementz et al.,  
343 2016; Drysdale et al., 2016; Mostert et al., 2018) or have mined transdiagnostic symptom dimensions  
344 underlying various psychiatric disorders (Grisanzio et al., 2017; Elliott et al., 2018; Xia et al., 2018a,  
345 b). Among studies examining the transdiagnostic symptom dimensions, most did not adopt a  
346 supervised machine learning predictive framework wherein the identified features along with the  
347 predictive algorithms are rigorously tested on unseen data. In addition, the differences in  
348 distance/similarity metrics used, coupled with the lack of ground truth in the unsupervised machine  
349 learning algorithms used to detect the transdiagnostic structure, make it difficult to validate the  
350 clinical utility of the identified features. We designed our study to overcome these limitations. To our  
351 best knowledge, our study is the first to use feature importance to guide forward model selection  
352 under a supervised machine learning framework to identify transdiagnostic psychopathological  
353 features across multiple DSM categories. The superior performance of our truncated models selected  
354 via the model selection approach demonstrate the clinical utility of the identified transdiagnostic  
355 features.

356 Though we built models with different modalities as inputs (e.g. personality traits, symptoms and  
357 neuroimaging), we found high performance models could be obtained without significant  
358 contribution of the imaging modalities. This finding contrasts with what would be predicted from the  
359 published literature. For example, a recent meta-analysis of studies on psychiatric disorders involving  
360 structural magnetic resonance imaging (sMRI) identified shared abnormalities in certain brain  
361 regions underlying common psychiatric disorders (Goodkind et al., 2015). In addition, studies using  
362 functional MRI (fMRI) found altered functional connectivity patterns shared across multiple  
363 categories of disorders such as SCZ, BD, and major depressive disorder (MDD) (Buckholtz and  
364 Meyer-Lindenberg, 2012; Wei et al., 2018). Similarly, another recent study focusing on MDD, post-  
365 traumatic stress disorder, and panic disorder identified 6 distinct subtypes based on 3 orthogonal  
366 symptom dimensions shared across the DSM diagnoses and their corresponding biomarkers in  
367 electroencephalogram (EEG) beta activity (Grisanzio et al., 2017). Although these studies did not  
368 systematically compare the predictability in each data modality, it is possible that the sample size in  
369 CNP or other methodological differences (e.g., parcellation used during sMRI and fMRI feature  
370 extraction) limited the weighted importance of structural or functional measures in our models.

371 A broad set of phenotypes from the self-report instruments were identified by our transdiagnostic  
372 classifiers to be shared across the patient populations. The phenotypes are distributed across all 13  
373 self-reported instruments and covers symptom domains encompassing personality and traits, positive  
374 and negative affect, cognition, sensory and social processing. For the top 20 most predictive features,  
375 mood dysregulation, impulsivity, inattention, neuroticism, social anhedonia and apathy weighted  
376 prominently in the transdiagnostic model. This high level of shared symptom domains across SCZ,  
377 BD, and ADHD is in line with recent genetic studies reporting significantly correlated risk factors for  
378 heritability among these three disorders (Larsson et al., 2013; The Brainstorm Consortium et al.,  
379 2017; Bipolar Disorder and Schizophrenia Working Group of the Psychiatric Genomics Consortium  
380 et al., 2018). For SCZ and BD, previous studies have identified shared features both in terms of  
381 symptoms and the underlying psychopathology and biology (Pearlson, 2015). Similarly, studies have  
382 identified shared symptoms and biology between SCZ and ADHD (Peralta et al., 2011; Park et al.,  
383 2018) and has found high levels of comorbidity between BD and ADHD along with the shared  
384 features between the two disorders (Nierenberg et al., 2005; Klassen et al., 2010; van Hulzen et al.,

385 2017; Wang et al., 2017). Despite these prior studies, the three diagnostic categories have not been  
386 considered together in a single study. Consistent with the findings reported in these studies, our study  
387 provides an important data-driven confirmation on the shared phenotypes and symptoms across the  
388 three disease categories.

389 Since the TCI is less commonly used in clinical practice and historically a greater emphasis has been  
390 placed on symptoms than personality traits, we were surprised by finding that the TCI contributed the  
391 largest proportion of questions among the set of 85 most predictive items determined by the  
392 transdiagnostic classifier. Prior studies have found that the personality traits and characters defined in  
393 the TCI are associated with various mood disorders (Cloninger et al., 1998; Grucza et al., 2003).  
394 Specifically, for disorders in the CNP dataset, studies have found positive association between  
395 personality dimensions characterized in TCI and overall ADHD symptom (Lynn et al., 2005;  
396 Anckarsäter et al., 2006) as well as subtypes of ADHD (Salgado et al., 2009). For SCZ, studies have  
397 identified links between positive and negative symptom dimensions and TCI factors (Guillem et al.,  
398 2002; Hori et al., 2008). Among BD patients, (Hajirezaei et al., 2017) identified personality profiles  
399 that are distinct from healthy controls and these profiles were further found to be shared with MDD.  
400 Since these studies associated disease symptoms solely with the known factor scores in the TCI, the  
401 contribution of the nuanced personality profiles captured in individual items in the TCI could not be  
402 determined. In the current study, the fact that we identified items in the TCI that corresponded to  
403 shared symptoms such as apathy, anhedonia, and distress directly extends prior literature and is  
404 consistent with studies documenting the relationship between TCI factor scores and symptoms such  
405 as anhedonia (Martinotti et al., 2008), as well as depression and anxiety (Jylhä and Isometsä, 2006).  
406 Additionally, prior studies only examined TCI's association with symptoms without simultaneously  
407 including other instruments as covariates in the model. This approach cannot evaluate the relative  
408 importance of the personality traits in TCI against the broader set of phenotypical features defined in  
409 other instruments. In this regard, our study established the usefulness of personality traits as a set of  
410 highly reliable transdiagnostic features among all features defined in the self-reported instruments in  
411 the CNP data.

412 The sum score of the 85 most predictive transdiagnostic items achieved much higher separability  
413 between HC and patients than known sub-scores and sum scores in the instruments that were  
414 specifically designed to assess diagnosis-specific symptom domains. This is true even for the subset  
415 of top 10 most predictive transdiagnostic items, which indicates that the shared phenotypic features  
416 across patient groups do not fully adhere to known dimensional structures in the instruments. Thus,  
417 using the total score and/or the sub-scores according to pre-defined subscales of a given instrument  
418 cannot identify the optimal set of transdiagnostic features. One explanation for this phenomenon is  
419 that because the patients share a broad range of phenotypic features, the pre-defined subscales and  
420 sum scores become insufficient in capturing the full dimensional structure since most of the  
421 instruments are designed to measure a limited set of constructs targeting a specific patient population  
422 (Avila et al., 2015). This further demonstrates the advantage of our importance-guided sequential  
423 model selection approach in identifying clinically relevant transdiagnostic features across a large set  
424 of instruments.

425 While patients shared a broad set of phenotypic features, our results showed deviations from this  
426 transdiagnostic structure within the most predictive features for each patient group. These differences  
427 may in particular reflect clustered personality traits and symptom domains that are most unique for  
428 each patient population. For SCZ, the unique features of perceptual aberration and psychological  
429 distress, along with other features that are consistent with the transdiagnostic structure, largely  
430 conform to the positive and negative symptom dimensions associative with SCZ patients. For BD,

431 the unique features of increased energy, physical anhedonia, and psychological distress serve to  
432 shape the symptom structure along the manic and depressive dimensions. For ADHD, the increased  
433 representation in inattention, hyperactivity, and impulsivity is consistent with the overall  
434 symptomatology of ADHD patients. Overall, the concurrent existence of shared and category-  
435 specific phenotypic features across the CNP patient groups is consistent with recent studies reporting  
436 both shared and distinct properties in functional brain networks (Grisanzio et al., 2017; Xia et al.,  
437 2018a, b) and genetic neuropathology (The Brainstorm Consortium et al., 2017; Gandal et al., 2018)  
438 across major psychiatric disorders. Our results raise the possibility of exploring the relationship  
439 between the predictive phenotypic features and the underlying genetics of the individuals or groups  
440 that present with these features.

441 In conclusion, we identified a set of transdiagnostic phenotypic features shared across SCZ, BD, and  
442 ADHD. This set of features distinguished the patient group from HC with high accuracy and a  
443 compact transdiagnostic screening scale can be derived from the corresponding top 10 most  
444 predictive questionnaire items. The feature importance guided sequential model selection provides a  
445 data-driven method to identify shared features under a supervised machine learning framework, in  
446 which the performance of the identified feature sets is evaluated on unseen data. This is an advantage  
447 over unsupervised machine learning methods. Moreover, the importance guided sequential model  
448 selection can be generalized to identify clinically-useful transdiagnostic features across categories  
449 defined in DSM-5 and ICD-10, or alternatively to identify the neural correlates of symptom severity  
450 across psychiatric disorders (Melleme et al., 2018). It should be noted that the medication status in the  
451 CNP dataset is not controlled. This suggests that although reliable transdiagnostic features could be  
452 identified across patient groups, the underlying cause of the observed symptom structure could  
453 potentially be confounded by the uncontrolled medication and symptom status. Future studies should  
454 further validate the transdiagnostic features identified in this study on other datasets with similar  
455 patient populations and with better controlled medication status. Including these additional datasets  
456 as out-of-sample validations can demonstrate the generalizability of the current results and  
457 methodology to the wider population.

458

## 459 **5 Conflict of Interest**

460 The authors are employees of BlackThorn Therapeutics, Inc, and are compensated financially by  
461 BlackThorn Therapeutics, Inc.

462

## 463 **6 Author Contributions**

464 YL, MM, HG, WM, PA designed the study; YL, MM, HG, MK, ARM, AM performed the analysis;  
465 YL, MM, HG, MK, ARM, WM, PA wrote the manuscript.

466

## 467 **7 Funding**

468 This work is funded by BlackThorn Therapeutics, Inc.

469

## 470 **8 Acknowledgments**

471 The authors would like to thank Clark Gao, Lori Jean Van Orden, Martine Meyer, and Simone  
472 Krupka for their help and discussions in shaping this work.

473

## 474 **9 References**

- 475 Abrams R., & Taylor M. (1981). Importance of schizophrenic symptoms in the diagnosis of mania.  
476 *Am J Psychiatry*, 138(5):658–661.
- 477 American Psychiatric Association. (2000). *Diagnostic and statistical manual of mental disorders*. (4th  
478 ed.). Washington, DC: American Psychiatric Press Inc.
- 479 Anckarsäter H., Stahlberg O., Larson T., Hakansson C., Jutblad S.B., Niklasson L., Nydén A., Wentz  
480 E., Westergren S., Cloninger C.R., Gillberg C., & Rastam M. (2006). The Impact of ADHD and  
481 autism spectrum disorders on temperament, character, and personality development. *Am J*  
482 *Psychiatry*, 163(7):1239–1244.
- 483 Avila M., Stinson J., Kiss A., Brandão L.R., Uleryk E., & Feldman B.M. (2015). A critical review of  
484 scoring options for clinical measurement tools. *BMC Res Notes* 8:612.
- 485 Bipolar Disorder and Schizophrenia Working Group of the Psychiatric Genomics Consortium.  
486 (2018). Genomic Dissection of Bipolar Disorder and Schizophrenia, Including 28 Subphenotypes.  
487 *Cell* 173(7):1705-1715.e16.
- 488 Brodersen K.H., Deserno L., Schlagenhaut F., Lin Z., Penny W.D., Buhmann J.M., & Stephan K.E.  
489 (2014). Dissecting psychiatric spectrum disorders by generative embedding. *Neuroimage Clin* 4:98–  
490 111.
- 491 Buckholtz J.W., & Meyer-Lindenberg A. (2012). Psychopathology and the human connectome:  
492 toward a transdiagnostic model of risk for mental illness. *Neuron* 74(6):990–1004.
- 493 Bzdok D., & Meyer-Lindenberg A. (2017). Machine Learning for Precision Psychiatry:  
494 Opportunities and Challenges. *Biol Psychiatry Cogn Neurosci Neuroimaging* 3(3):223-230.
- 495 Clementz B.A., Sweeney J.A., Hamm JP, Ivleva EI, Ethridge LE, Pearlson GD, Keshavan MS, &  
496 Tamminga CA (2016) Identification of Distinct Psychosis Biotypes Using Brain-Based Biomarkers.  
497 *Am J Psychiatry* 173(4):373–384.
- 498 Cloninger CR, Bayon C, & Svrakic DM (1998) Measurement of temperament and character in mood  
499 disorders: a model of fundamental states as personality types. *J Affect Disorder* 51(1):21–32.
- 500 Coryell W, Leon AC, Turvey C, Akiskal HS, Mueller T, & Endicott J (2001) The significance of  
501 psychotic features in manic episodes: a report from the NIMH collaborative study. *J Affect Disord*  
502 67(1-3):79–88.
- 503 Cross-Disorder Group of the Psychiatric Genomics Consortium (2013) Identification of risk loci with  
504 shared effects on five major psychiatric disorders: a genome-wide analysis. *Lancet* 381(9875):1371–  
505 1379.
- 506 Desikan RS, Ségonne F, Fischl B, Quinn BT, Dickerson BC, Blacker D, Buckner RL, Dale AM,  
507 Maguire PR, Hyman BT, Albert MS, & Killiany RJ (2006) An automated labeling system for  
508 subdividing the human cerebral cortex on MRI scans into gyral based regions of interest.  
509 *Neuroimage* 31(3):968–980.

- 510 Costa Dias TG, Iyer SP, Carpenter SD, Cary RP, Wilson VB, Mitchell SH, Nigg JT, & Fair DA  
511 (2015) Characterizing heterogeneity in children with and without ADHD based on reward system  
512 connectivity. *Dev Cogn Neurosci* 11:155–174.
- 513 Doshi-Velez F, Ge Y, & Kohane I (2014) Comorbidity clusters in autism spectrum disorders: an  
514 electronic health record time-series analysis. *Pediatrics* 133(1):e54–63.
- 515 Drysdale AT, Grosenick L, Downar J, Dunlop K, Mansouri F, Meng Y, ... Liston C (2016) Resting-  
516 state connectivity biomarkers define neurophysiological subtypes of depression. *Nat Med* 23(1):28-  
517 38.
- 518 Elliott ML, Romer AL, Knodt AR, & Hariri AR (2018) A Connectome-Wide Functional Signature of  
519 Transdiagnostic Risk for Mental Illness. *Biol Psychiat* 84(6):452-459.
- 520 First, M. B., Spitzer, R. L., Gibbon, M. & Williams, J. B.W. Structured Clinical Interview for DSM-  
521 IV-TR Axis I Disorders, Research Version, Patient Edition. (SCID-I/P) (2002).
- 522 Fischl B, Liu A, Dale AM (2001) Automated Manifold Surgery: Constructing Geometrically  
523 Accurate and Topologically Correct Models of the Human Cerebral Cortex. *IEEE Trans Med*  
524 *Imaging* 20:70.
- 525 Fischl B, Salat DH, Busa E, Albert M, Dieterich M, Haselgrove C, van der Kouwe A, Killiany R,  
526 Kennedy D, Klaveness S, Montillo A, Makris N, Rosen B, Dale AM (2002) Whole Brain  
527 Segmentation Automated Labeling of Neuroanatomical Structures in the Human Brain. *Neuron*  
528 33:341–355.
- 529 Gandal MJ, Haney JR, Parikshak NN, Leppa V, Ramaswami G, Hartl C, Schork AJ, Appadurai V,  
530 Buil A, Werge TM, Liu C, White KP, Consortium C, Consortium P, Group iPSYCH-B, Horvath S,  
531 Geschwind DH (2018) Shared molecular neuropathology across major psychiatric disorders parallels  
532 polygenic overlap. *Science* 359:693–697.
- 533 Geisler D, Walton E, Naylor M, Roessner V, Lim KO, Schulz CS, Gollub RL, Calhoun VD,  
534 Sponheim SR, Ehrlich S (2015) Brain structure and function correlates of cognitive subtypes in  
535 schizophrenia. *Psychiatry Res Neuroimaging* 234:74–83.
- 536 Georgiades S, Szatmari P, Boyle M, Hanna S, Duku E, Zwaigenbaum L, Bryson S, Fombonne E,  
537 Volden J, Mirenda P, Smith I, Roberts W, Vaillancourt T, Waddell C, Bennett T, Thompson A, in  
538 Team P (2013) Investigating phenotypic heterogeneity in children with autism spectrum disorder: a  
539 factor mixture modeling approach. *J Child Psychol Psych* 54:206–215.
- 540 Gheiratmand M, Rish I, Cecchi GA, Brown MR, Greiner R, Polosecki PI, Bashivan P, Greenshaw  
541 AJ, Ramasubbu R, Dursun SM (2017) Learning stable and predictive network-based patterns of  
542 schizophrenia and its clinical symptoms. *Npj Schizophrenia* 3:22.
- 543 Goodkind M, Eickhoff SB, Oathes DJ, Jiang Y, Chang A, Jones-Hagata LB, Ortega BN, Zaiko YV,  
544 Roach EL, Korgaonkar MS, Grieve SM, Galatzer-Levy I, Fox PT, Etkin A (2015) Identification of a  
545 Common Neurobiological Substrate for Mental Illness. *JAMA Psychiatry* 72:305–315.
- 546 Grisanzio KA, Goldstein-Piekarski AN, Wang M, Ahmed AP, Samara Z, Williams LM (2017)  
547 Transdiagnostic Symptom Clusters and Associations With Brain, Behavior, and Daily Function in  
548 Mood, Anxiety, and Trauma Disorders. *JAMA Psychiatry* 75(2):201-209.
- 549 Grucza RA, Przybeck TR, Spitznagel EL, Cloninger CR (2003) Personality and depressive  
550 symptoms: a multi-dimensional analysis. *J Affect Disorders* 74:123–130.
- 551 Guillem F, Bicu M, Semkovska M, Debruille JB (2002) The dimensional symptom structure of  
552 schizophrenia and its association with temperament and character. *Schizophr Res* 56:137–147.

- 553 Hajirezaei S, Mohammadi A, Soleimani M, Rahiminezhad F, Mohammadi M, Cloninger RC (2017)  
554 Comparing the Profile of Temperament and Character Dimensions in Patients with Major Depressive  
555 Disorder and Bipolar Mood Disorder with a Control Group. *Iranian J Psychiatry* 12:147–153.
- 556 Hamshere ML, Stergiakouli E, Langley K, Martin J, Holmans P, Kent L, Owen MJ, Gill M, Thapar  
557 A, O'Donovan M, Craddock N (2013) Shared polygenic contribution between childhood attention-  
558 deficit hyperactivity disorder and adult schizophrenia. *Br J Psychiatry* 203:107–111.
- 559 Hori H, Noguchi H, Hashimoto R, Nakabayashi T, Saitoh O, Murray RM, Okabe S, Kunugi H (2008)  
560 Personality in schizophrenia assessed with the Temperament and Character Inventory (TCI). *Psychiat  
561 Res* 160:175–183.
- 562 Jo H, Saad ZS, Simmons KW, Milbury LA, Cox RW (2010) Mapping sources of correlation in  
563 resting state fMRI, with artifact detection and removal. *Neuroimage* 52:571–582.
- 564 Jylhä P, Isometsä E (2006) Temperament, character and symptoms of anxiety and depression in the  
565 general population. *Eur Psychiat* 21(6):389-395.
- 566 Kaufman, J., Birmaher, B., Brent, D. A., Ryan, N. D. & Rao, U. (2000). K-SADS-PL. *J Am Acad  
567 Child Adolesc Psychiatry* 39(10): 1208.
- 568 Keck PE, McElroy SL, Havens J, Altshuler LL, Nolen WA, Frye MA, Suppes T, Denicoff KD,  
569 Kupka R, Leverich GS, Rush AJ, Post RM (2003) Psychosis in bipolar disorder: phenomenology and  
570 impact on morbidity and course of illness. *Compr Psychiat* 44:263–269.
- 571 Kessler R, Gruber M, Hettema J, Hwang I, Sampson N, Yonkers K (2007) Co-morbid major  
572 depression and generalized anxiety disorders in the National Comorbidity Survey follow-up. *Psychol  
573 Med* 38:365–374.
- 574 Kessler RC, Demler O, Frank RG, Olfson M, Pincus H, Walters EE, Wang P, Wells KB, Zaslavsky  
575 AM (2005) Prevalence and Treatment of Mental Disorders, 1990 to 2003. *New Engl J Medicine*  
576 352:2515–2523.
- 577 Klassen LJ, Katzman MA, Chokka P (2010) Adult ADHD and its comorbidities, with a focus on  
578 bipolar disorder. *J Affect Disorders* 124:1–8.
- 579 Krueger RF, Markon KE (2006) Reinterpreting Comorbidity: A Model-Based Approach to  
580 Understanding and Classifying Psychopathology. *Annu Rev Clin Psycho* 2:111–133.
- 581 Krueger RF, Markon KE (2011) A Dimensional-Spectrum Model of Psychopathology: Progress and  
582 Opportunities. *Arch Gen Psychiat* 68:10–11.
- 583 Lamers F, Burstein M, He J, Avenevoli S, Angst J, Merikangas KR (2012) Structure of major  
584 depressive disorder in adolescents and adults in the US general population. *Br J Psychiatry* 201:143–  
585 150.
- 586 Larsson H, Rydén E, Boman M, Långström N, Lichtenstein P, Landén M (2013) Risk of bipolar  
587 disorder and schizophrenia in relatives of people with attention-deficit hyperactivity disorder. *Br J  
588 Psychiatry* 203:103–106.
- 589 Lewandowski K, Sperry S, Cohen B, Öngür D (2014) Cognitive variability in psychotic disorders: a  
590 cross-diagnostic cluster analysis. *Psychol Med* 44:3239–3248.
- 591 Lotan A, Michaela Fenckova , Janita Bralten, Aet Alittoa, Luanna Dixson, Robert W. Williams and  
592 Monique van der Voet (2014) Neuroinformatic analyses of common and distinct genetic components  
593 associated with major neuropsychiatric disorders. *Frontiers in Neuroscience* 8: 1-15.

- 594 Lynn DE, Lubke G, Yang M, McCracken JT, McGough JJ, Ishii J, Loo SK, Nelson SF, Smalley SL  
595 (2005) Temperament and Character Profiles and the Dopamine D4 Receptor Gene in ADHD. *Am J*  
596 *Psychiat* 162:906–913.
- 597 Markon K (2009) Modeling psychopathology structure: a symptom-level analysis of Axis I and II  
598 disorders. *Psychol Med* 40:273–288.
- 599 Martinotti G, Cloninger CR, Janiri L (2009) Temperament and character inventory dimensions and  
600 anhedonia in detoxified substance-dependent subjects. *Am J Drug Alcohol Abus* 34(2):177-183.
- 601 Mellem SM, Liu Y, Gonzalez H, Kollada M, Martin WJ, Ahammad P (2018) Machine learning  
602 models identify multimodal measurements highly predictive of transdiagnostic symptom severity for  
603 mood, anhedonia, and anxiety. *BioRxiv*, doi: <https://doi.org/10.1101/414037>
- 604 Mostert JC, Hoogman M, Onnink MA, van Rooij D, von Rhein D, van Hulzen KJ, Dammers J, Kan  
605 CC, Buitelaar JK, Norris DG, Franke B (2018) Similar Subgroups Based on Cognitive Performance  
606 Parse Heterogeneity in Adults with ADHD and Healthy Controls. *J Atten Disord* 22:281–292.
- 607 Nierenberg AA, Miyahara S, Spencer T, Wisniewski SR, Otto MW, Simon N, Pollack MH, Ostacher  
608 MJ, Yan L, Siegel R, Sachs GS, Investigators S-B (2005) Clinical and Diagnostic Implications of  
609 Lifetime Attention-Deficit/Hyperactivity Disorder Comorbidity in Adults with Bipolar Disorder:  
610 Data from the First 1000 STEP-BD Participants. *Biol Psychiat* 57:1467–1473.
- 611 Ojala M, Garriga GC (2009) Permutation Tests for Studying Classifier Performance. 2009 Ninth Ieee  
612 *Int Conf Data Min*:908–913.
- 613 Pacheco A, Barguil M, Contreras J, Montero P, Dassori A, Escamilla MA, Raventós H (2010) Social  
614 and clinical comparison between schizophrenia and bipolar disorder type I with psychosis in Costa  
615 Rica. *Soc Psych Psych Epid* 45:675–680.
- 616 Park MM, Raznahan A, Shaw P, Gogtay N, Lerch JP, Chakravarty MM (2018) Neuroanatomical  
617 phenotypes in mental illness: identifying convergent and divergent cortical phenotypes across autism,  
618 ADHD and schizophrenia. *J Psychiatry Neurosci* 43:201–212.
- 619 Pearlson GD (2015) Etiologic, Phenomenologic, and Endophenotypic Overlap of Schizophrenia and  
620 Bipolar Disorder. *Annu Rev Clin Psycho* 11:1–31.
- 621 Peralta V, de Jalón E, Campos MS, Zandío M, Sanchez-Torres A, Cuesta MJ (2011) The meaning of  
622 childhood attention-deficit hyperactivity symptoms in patients with a first-episode of schizophrenia-  
623 spectrum psychosis. *Schizophr Res* 126:28–35.
- 624 Poldrack RA, Congdon E, Triplett W, Gorgolewski KJ, Karlsgodt KH, Mumford JA, Sabb FW,  
625 Freimer NB, London ED, Cannon TD, Bilder RM (2016) A phenome-wide examination of neural  
626 and cognitive function. *Sci Data* 3:sdata2016110.
- 627 Pope HG, Lipinski JF (1978) Diagnosis in Schizophrenia and Manic-Depressive Illness: A  
628 Reassessment of the Specificity of “Schizophrenic” Symptoms in the Light of Current Research.  
629 *Arch Gen Psychiat* 35:811–828.
- 630 Power JD, Cohen AL, Nelson SM, Wig GS, Barnes K, Church JA, Vogel AC, Laumann TO, Miezin  
631 FM, Schlaggar BL, Petersen SE (2011) Functional Network Organization of the Human Brain.  
632 *Neuron* 72:665–678.
- 633 Purcell SM et al. (2009) Common polygenic variation contributes to risk of schizophrenia and  
634 bipolar disorder. *Nature* 460:748.

- 635 Rhebergen D, Lamers F, Spijker J, de Graaf R, Beekman A, Penninx B (2011) Course trajectories of  
636 unipolar depressive disorders identified by latent class growth analysis. *Psychol Med* 42:1383–1396.
- 637 Ryali S, Chen T, Supekar K, Menon V (2012) Estimation of functional connectivity in fMRI data  
638 using stability selection-based sparse partial correlation with elastic net penalty. *Neuroimage*  
639 59:3852–3861.
- 640 Salgado CAI, Bau CHD, Grevet EH, Fischer AG, Victor MM, Kalil KLS, Sousa NO, Garcia CR,  
641 Belmonte-de-Abreu P (2009) Inattention and Hyperactivity Dimensions of ADHD Are Associated  
642 with Different Personality Profiles. *Psychopathology* 42:108–112.
- 643 Sun H, Lui S, Yao L, Deng W, Xiao Y, Zhang W, Huang X, Hu J, Bi F, Li T, Sweeney JA, Gong Q  
644 (2015) Two Patterns of White Matter Abnormalities in Medication-Naive Patients with First-Episode  
645 Schizophrenia Revealed by Diffusion Tensor Imaging and Cluster Analysis. *JAMA Psychiatry*  
646 72:678–686.
- 647 The Brainstorm Consortium et al. (2017). Analysis of shared heritability in common disorders of the  
648 brain. *Science*, 360 (6395):eaap8757.
- 649 van Hulst B, de Zeeuw P, Durston S (2014) Distinct neuropsychological profiles within ADHD: a  
650 latent class analysis of cognitive control, reward sensitivity and timing. *Psychol Med* 45:735–745.
- 651 van Hulzen K, Scholz CJ, Franke B, Ripke S, Klein M, McQuillin A, Sonuga-Barke EJ, Group P,  
652 Kelsoe JR, Landén M, Andreassen OA, Group P, Lesch K-P, Weber H, Faraone SV, Arias-Vasquez  
653 A, Reif A (2017) Genetic Overlap Between Attention-Deficit/Hyperactivity Disorder and Bipolar  
654 Disorder: Evidence from Genome-wide Association Study Meta-analysis. *Biol Psychiat* 82:634–641.
- 655 van Loo HM et al. (2014) Major depressive disorder subtypes to predict long-term course. *Depress*  
656 *Anxiety* 31:765–777.
- 657 van Loo HM, de Jonge P, Romeijn J-W, Kessler RC, Schoevers RA (2012) Data-driven subtypes of  
658 major depressive disorder: a systematic review. *Bmc Med* 10:1–12.
- 659 Veatch O, Veenstra V, VanderWeele J, Potter M, Pericak Vance M, Haines J (2014) Genetically  
660 meaningful phenotypic subgroups in autism spectrum disorders. *Genes Brain Behav* 13:276–285.
- 661 Wang H, Jung Y-E, Chung S-K, Hong J, Kang N, Kim M-D, Bahk W-M (2017) Prevalence and  
662 correlates of bipolar spectrum disorder comorbid with ADHD features in nonclinical young adults. *J*  
663 *Affect Disorders* 207:175–180.
- 664 Wei Y, Chang M, Womer FY, Zhou Q, Yin Z, Wei S, Zhou Y, Jiang X, Yao X, Duan J, Xu K, Zuo  
665 X-N, Tang Y, Wang F (2018) Local functional connectivity alterations in schizophrenia, bipolar  
666 disorder, and major depressive disorder. *J Affect Disorders* 236:266–273.
- 667 Xia C.H. et al. (2018a) Linked dimensions of psychopathology and connectivity in functional brain  
668 networks. *Nat Commun* 9(1):3003.
- 669 Xia M, Womer FY, Chang M, Zhu Y, Zhou Q, Edmiston EK, Jiang X, Wei S, Duan J, Xu K, Tang  
670 Y, He Y, Wang F (2018b) Shared and Distinct Functional Architectures of Brain Networks Across  
671 Psychiatric Disorders. *Schizophr Bull*. doi: 10.1093/schbul/sby046
- 672 Zou H, Hastie T (2005) Regularization and variable selection via the elastic net. *J Royal Statistical*  
673 *Soc Ser B Statistical Methodol* 67:301–320.



**Table 1. Demographic Information\***

	<b>HC</b>	<b>SCZ</b>	<b>BD</b>	<b>ADHD</b>	<b>Total</b>
No. of subjects	130	50	49	43	272
With complete phenotype data	130	50	48	43	271
With sMRI data**	98	30	44	34	206
With fMRI data <sup>†</sup>	104	47	41	37	229
<b>Age</b>					
Mean age	31.26	36.46	35.15	33.09	
SD age	8.74	8.88	9.07	10.76	
Range age	21-50	22-49	21-50	21-50	
<b>Gender</b>					
No. of female subjects	62	12	21	22	
Percent female subjects	47.69%	24.00%	42.86%	51.16%	
<b>Race</b>					
American Indian or Alaskan Native	19.23%	22.00%	6.25%	0%	
Asian	15.38%	2.00%	0%	2.33%	
Black/African American	0.77%	4.00%	2.08%	2.33%	
White	78.46%	66.00%	77.08%	88.37%	
More than one race	0%	2.00%	14.58%	6.98%	
<b>Education</b>					
No high school	1.54%	18.00%	2.08%	0%	
High school	12.31%	44.00%	29.17%	23.26%	
Some college	20.77%	18.00%	25.00%	30.23%	
Associate's degree	7.69%	4.00%	6.25%	6.98%	
Bachelor's degree	50.00%	10.00%	29.17%	32.56%	
Graduate degree	6.92%	0%	4.17%	2.33%	
Other	0.77%	4.00%	4.17%	4.65%	

\* Demographic information is based on initial number of subjects

\*\* Excluding subjects with aliasing artifacts

<sup>†</sup> Excluding subjects with misaligned structural-function imaging data

**Table 2. Performances of the transdiagnostic models on each feature set\***

**Performance of the full model:**

	Scales	sMRI	fMRI	s+fMRI	Scales+sMRI	Scales+fMRI	Scales+s+fMRI
AUC	0.83(0.04)	0.56(0.05)	0.59(0.04)	0.57(0.05)	0.89(0.07)	0.86(0.06)	0.86(0.05)
Accuracy	0.77(0.05)	0.58(0.08)	0.60(0.06)	0.61(0.07)	0.91(0.04)	0.87(0.05)	0.86(0.05)
Sensitivity	0.77(0.07)	0.74(0.11)	0.60(0.11)	0.62(0.11)	0.86(0.08)	0.82(0.12)	0.86(0.08)
Specificity	0.82(0.07)	0.38(0.11)	0.56(0.12)	0.49(0.17)	0.80(0.15)	0.61(0.30)	0.48(0.26)

**Performance of the best truncated model:**

	Scales	sMRI	fMRI	s+fMRI	Scales+sMRI	Scales+fMRI	Scales+s+fMRI
AUC	0.95(0.02)	0.78(0.06)	0.87(0.08)	0.77(0.06)	0.96(0.03)	0.98(0.02)	0.96(0.03)
Accuracy	0.88(0.04)	0.71(0.06)	0.85(0.07)	0.77(0.06)	0.87(0.05)	0.92(0.04)	0.90(0.04)
Sensitivity	0.87(0.08)	0.81(0.09)	0.86(0.09)	0.77(0.08)	0.93(0.07)	0.91(0.06)	0.94(0.05)
Specificity	0.88(0.04)	0.60(0.16)	0.84(0.18)	0.76(0.07)	0.80(0.15)	0.92(0.04)	0.85(0.09)
No. of features	85	131	8192	16384	238	32	64

**Test on AUCs between the full and the truncated model\*\*:**

	Scales	sMRI	fMRI	s+fMRI	Scales+sMRI	Scales+fMRI	Scales+s+fMRI
Test statistic	100	100	100	99.5	82.5	100	95
p-value	< 0.001	< 0.001	< 0.001	< 0.001	0.01537	< 0.001	< 0.001

\* The mean performance measures across 10 implementations are reported here with the standard deviation shown in parentheses

\*\* Wilcoxon's rank-sum test

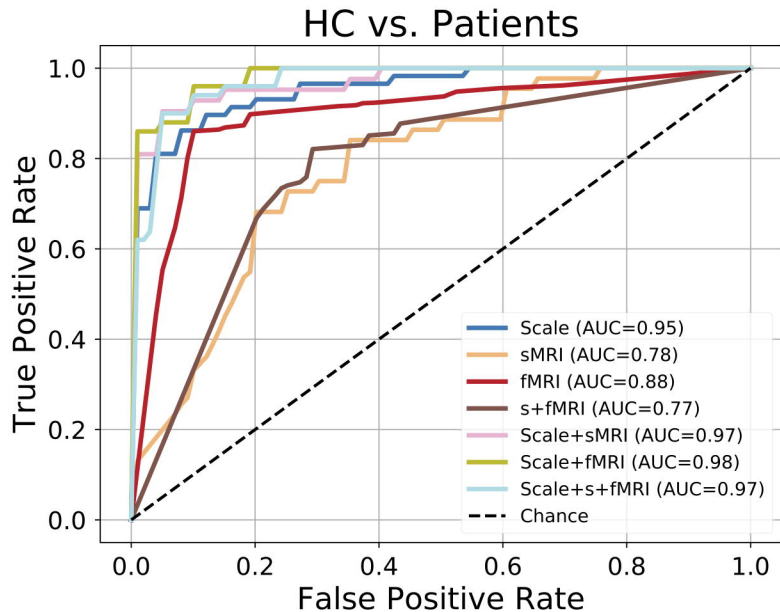
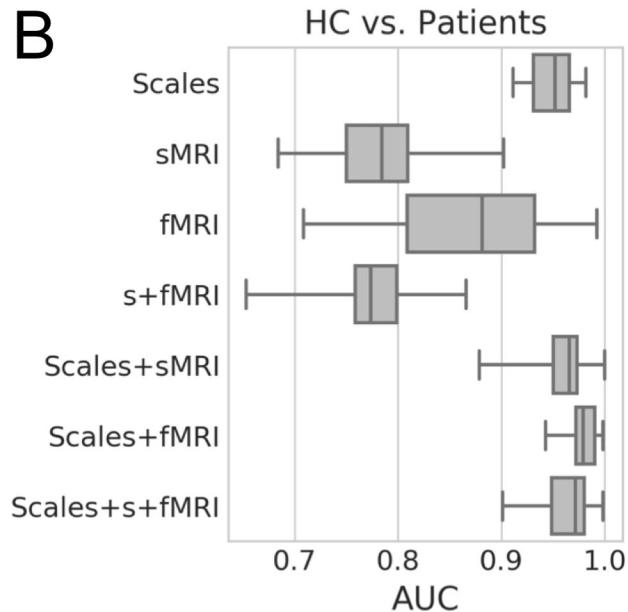
## Figure Legends

**Figure 1.** The performances of the best transdiagnostic models selected via the feature importance-guided sequential model selection procedure. **A)** The receiver operating characteristic (ROC) curve for the best truncated models based on each feature set. Area under the ROC curve (AUC) for each model is listed in the legend. **B)** Box plots showing the AUC of the best truncated model for each feature set measured across 10 implementations of sequential model selection procedure.

**Figure 2.** Distributions and effect sizes of the model's derived scores vs. the existing scale scores. **A)** Sum score calculated from the identified 85 most predictive items showing high separability in terms of Cohen's  $d$  between HC and Patients. **B)** All three patient categories showed elevated sum scores relative to HC ( $p < 0.001$ ). **C)** The 4 temperament sub-scores in TCI included in the CNP dataset showing only medium effect sizes between HC and Patients. **D)** Box plot showing significantly higher effect size from the identified 85 items (asterisk) compared to all predefined sum and subscores in self-reported instruments in CNP data. The asterisk represents the Cohen's  $d$  between HC and Patients from the top 85 items, whereas the box plot shows the effect sizes from all predefined sum and subscores (also see Supplementary Table 1).

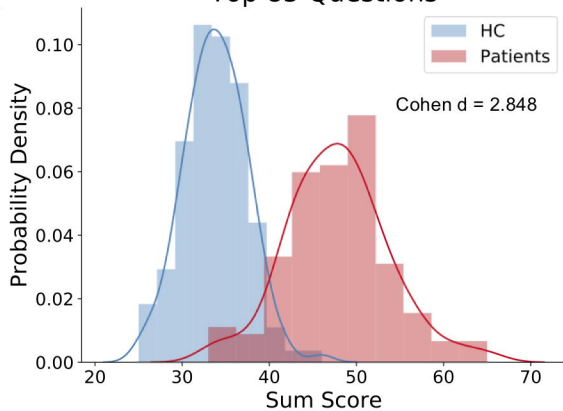
**Figure 3.** The percentage of items from each of the 13 self-reported instruments among the set of 85 most predictive transdiagnostic items.

**Figure 4.** The grouping of items into specific phenotypic domains for the top 20 most predictive items from **A)** the HC vs. All Patients transdiagnostic model and **B) – D)** the 3 HC vs. a single patient category classifiers. The radius in the spider plots represents item counts.

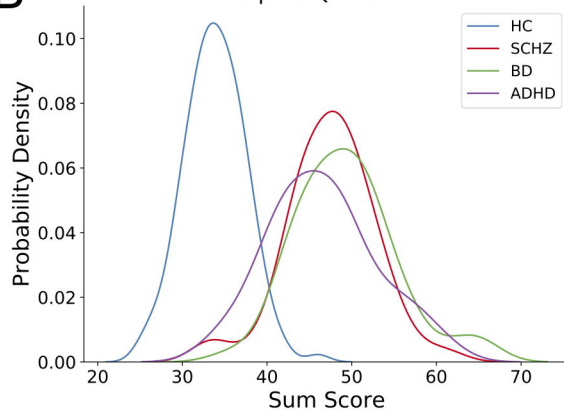
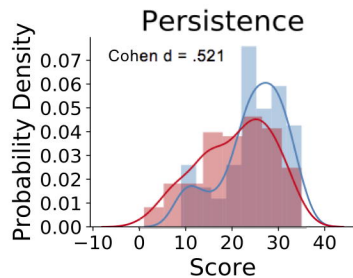
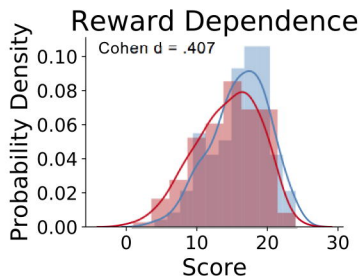
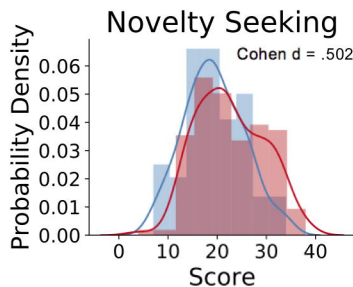
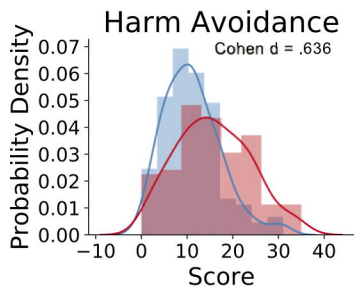
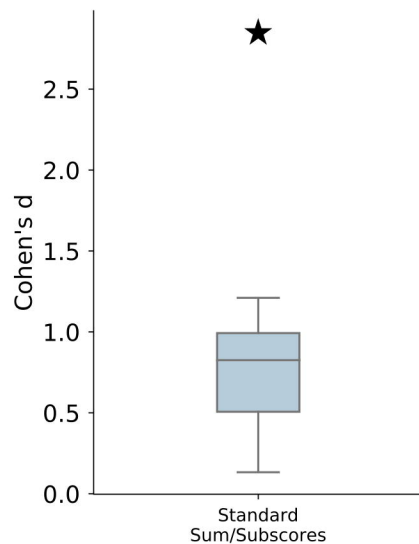
**A****B**

**A**

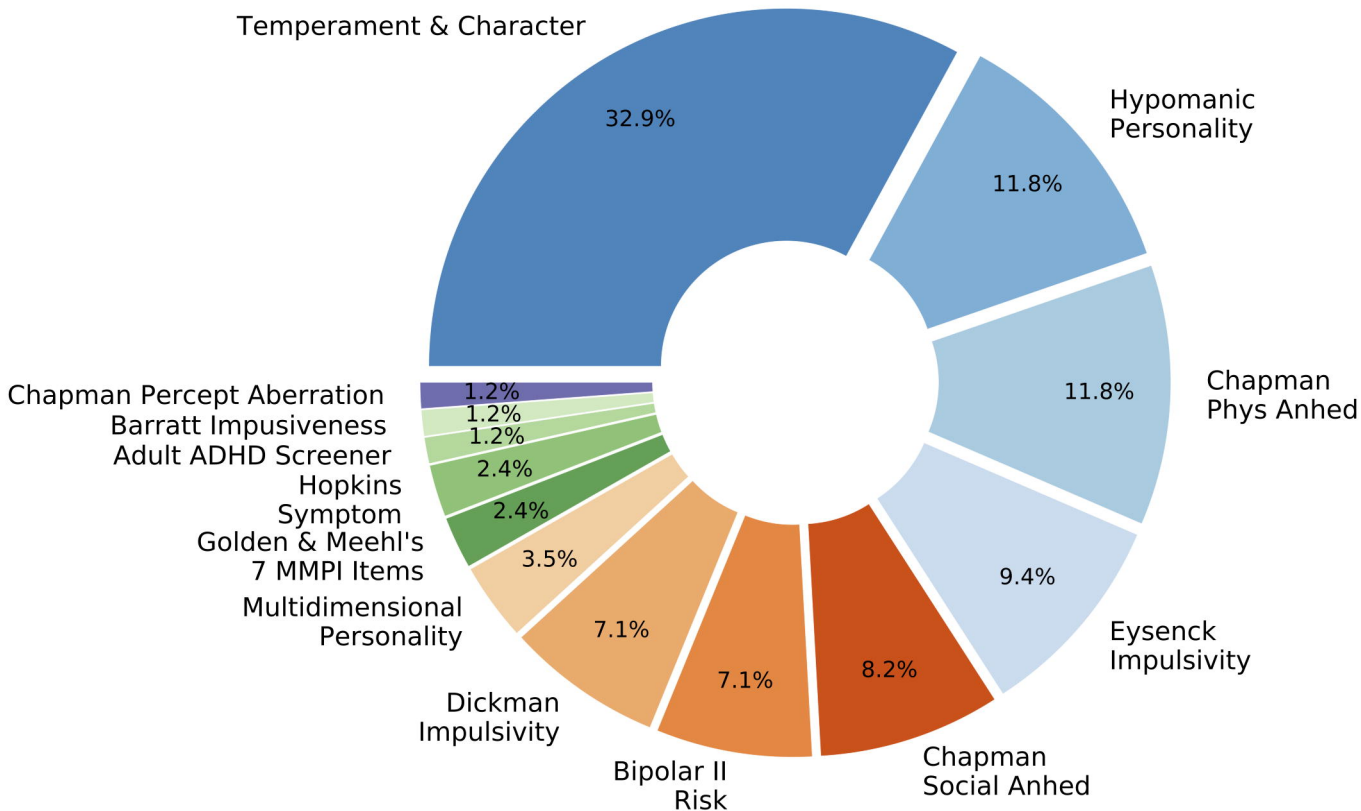
## Top 85 Questions

**B**

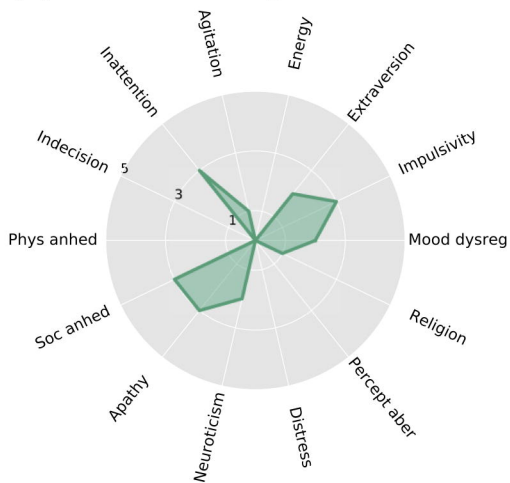
## Top 85 Questions

**C****D**

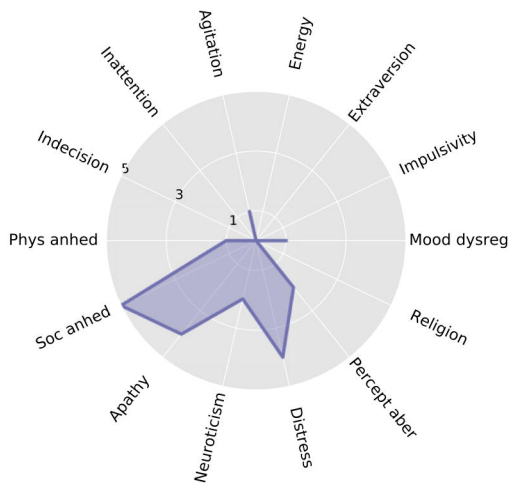
# Temperament & Character



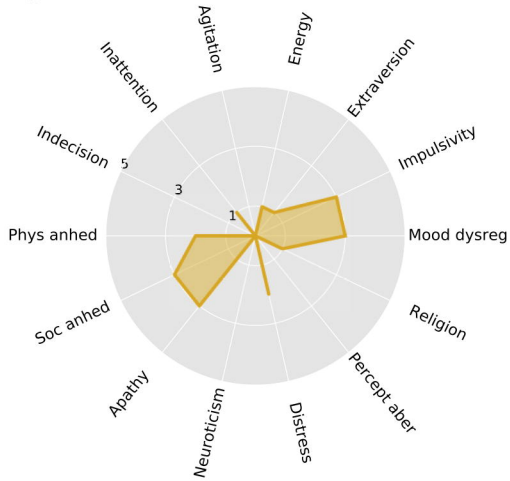
# A Transdiagnostic



# B SCZ



# C BD



# D ADHD

